

## Estimation of land surface temperature of Srinagar city, India using Landsat 8 data.

### Estimación de la temperatura de la superficie terrestre de la ciudad de Srinagar, India utilizando datos de Landsat 8.

Perminder Singh<sup>1,\*</sup>, Dr. Sandeep Singla<sup>2</sup>

<sup>1</sup> Research Scholar at Rimt University Mandi Gobindgarh , Punjab-147301, India.

<sup>2</sup> Prof. Civil Engineering Department Rimt University Mandi Gobindgarh , Punjab-147301

\* Author for correspondence, email: [perminder035@gmail.com](mailto:perminder035@gmail.com)

#### ABSTRACT

Land surface temperature (LST) is a critical parameter for the study of biosphere, cryosphere and climate change. Thermal infrared remote sensing data can be used to measure Land Surface Temperature (LST). It will measure the energy exiting the Earth's surface and record the apparent temperature of the surface. It is now possible to measure LST due to the advent of satellite imagery and digital image processing applications. In this study an attempt has been made to estimate LST over Srinagar city India, using LANDSAT 8 – Operational Line Imager & Thermal Infrared Sensor (OLI & TIRS) satellite data. The variability of retrieved LSTs has been investigated with respect to Normalized Difference Vegetation Index (NDVI). The LST for Srinagar city was calculated using the Split Window algorithm (SW) and Landsat-8 (Path-149 and Row-36) Thermal Infrared Sensor (TIRS) data with a resolution of 100m. Emissivity was calculated using the Normalized Differential Vegetation Index (NDVI) proportion of vegetation methodology, with bands 4 and 5 (30 m resolution) from the Operational Land Imager (OLI). Surface temperatures were found to be higher in central regions and lower in heavily vegetated areas. The LST derived using the SW algorithm was more efficient and precise since it used both OLI and TIRS bands.

Keywords: Land surface temperature (LST), Normalized Differential Vegetation Index (NDVI), Thermal Infrared Sensor (TIRS)

#### Resumen

La temperatura de la superficie terrestre (LST) es un parámetro crítico para el estudio de la biosfera, la criosfera y el cambio climático. Los datos de teledetección infrarroja térmica se pueden utilizar para medir la temperatura de la superficie terrestre (LST). Medirá la

energía que sale de la superficie de la Tierra y registrará la temperatura aparente de la superficie. Ahora es posible medir LST debido a la llegada de imágenes de satélite y aplicaciones de procesamiento de imágenes digitales. En este estudio se ha intentado estimar LST sobre la ciudad de Srinagar, India, utilizando datos de satélite LANDSAT 8 - Sensor de imagen de línea operativa y sensor de infrarrojos térmicos (OLI & TIRS). La variabilidad de los LST recuperados se ha investigado con respecto al Índice de vegetación de diferencia normalizada (NDVI). El LST para la ciudad de Srinagar se calculó utilizando el algoritmo de ventana dividida (SW) y el sensor infrarrojo térmico Landsat-8 (Path-149 y Row-36) (TIRS) con una resolución de 100 m. . La emisividad se calculó utilizando la metodología de proporción de vegetación del Índice de Vegetación Diferencial Normalizado (NDVI), con bandas 4 y 5 (resolución de 30 m) del Operational Land Imager (OLI). Se encontró que las temperaturas de la superficie eran más altas en las regiones centrales y más bajas en las áreas densamente vegetadas. El LST derivado usando el algoritmo SW fue más eficiente y preciso ya que usó bandas OLI y TIRS.

Palabras clave: temperatura de la superficie terrestre (LST), índice de vegetación diferencial normalizado (NDVI), sensor infrarrojo térmico (TIRS)

## INTRODUCTION

For thousands of years, human induced activity has changed our planet earth and its climate. The high demographic pressure, relocation and socio-economic practices intensify these environmental changes. This transitions were observed at different spatial levels from local to global. (Mahmood R et al., 2010; Rajeshwari et.al, 2014) Remote Sensing (RS) and Geographic Information Systems (GIS) have nearly doubled human ability to view the planet by means of sensors to observation of complex shifts on Earth's surface. The environmental and climatic aspects of the different applications of geoscience and natural resource management are especially well understood by RS and GIS (Alam et al., 2017; Kannaujiya et al., 2020; Kothyari et al., 2019;) The LST is the Earth's surface temperature and the interface temperature between the earth's surface and atmosphere (Malik and Shukla, 2018; Singh et al., 2020). Land surface temperature(LST) is a critical factor controlling the chemical, physical, and biological processes of earth systems (Liu et al.2006; Mallick et al.2008; Tan et al. 2010; Grigsby et al.2015). LST has been a significant used over the years in the field of agricultural research, evapotranspiration, climate change, the hydrological cycle, forest fires, , vegetation monitoring, urban climate, heating urban islands and volcanic studies (Arnfield2003; Bastiaanssen et al.1998; Hansen et al.2010; Kalma et al.2008; Kogan2001;Su 2002; Voogt and Oke2003; Weng 2009; Weng et al.2004), (Fisher. et al., 2017; Niclos et al., 2009). Thermal images can be retrieved using the single infrared

channel system or the split window process, depending on the number of bands used (Pu et al., 2006 LST varies on evaporating and non-evaporating surfaces along urban-rural gradient... Temperature and emissivity are the primary variables to determine, in accordance with the law of Planck, how much thermal infrared energy is radiated from Earth's surface. These variables will provide information of many different types of Earth surface processes, surface-atmosphere interactions and evapo-transpiration (Anderson et al., 2011). The emissivity of the material's surface is its efficiency in the emission of energy as a thermal radiation, which measures black body radiance to anticipate the emitted radiation. The soil structure, the composition of the soil, organic matter, moisture content and vegetative cover properties are determined (Van De Griend and Owe, 1993; Jin and Liang, 2006; Malik and Shukla et al., 2018), The studies by Yuan and Bauer (2007) and Xiong et al. (2012) revealed high LST in dense built up areas having high concentration of population. Landsat-8 is equipped with two sensors, i.e., the operational land imager (OLI) and the thermal infrared sensor (TIRS). OLI collects data in the visible, near infrared and in the short-wave, electromagnetic spectrum infrared regions with a spatial resolution of 30 m, plus an additional panchromatic band at 15 m spatial resolution. The TIRS sensor uses two bands in the atmospheric window between 10 and 12 to calculate 100 m spatial resolution of TIR's radiance. (Irons et al. 2012). For the LST retrieval, we firstly present the computation of the brightness temperature. Secondly, we estimate the required parameters (atmospheric transmittance, land surface emissivity and atmospheric water vapour content) for the SW algorithm.

## MATERIAL AND METHODS

Study Area: Srinagar City is situated between Latitudes and Longitudes of 33°53'49"-34° 17'14"N and 74°36'16"- 75°01'26"E. It is located in the middle of the oval Kashmir valley, at an altitude of 1585 meters above sea level. The study area spreads between the plains of valley of Kashmir along the river Jhelum.. The Jhelum River swirls through the city centre.. The natural wall of mountains is surrounding both the city and its interior (the sub-mountain branches of the PirPanjal range). The district is alluvial filled basin similar to the valley, the karewas formation in the valley belong to Pleistocene and post Pleistocene age having horizontally stratified depositions of lacustrine origin beds of sand. The Srinagar City is spread across an area of 292 km<sup>2</sup>. Srinagar City has a humid subtropical climate (KöppenCfa) according to Köppen. The City has a sub-Mediterranean climate with harsh winters and mild summers with a comparatively high humidity.

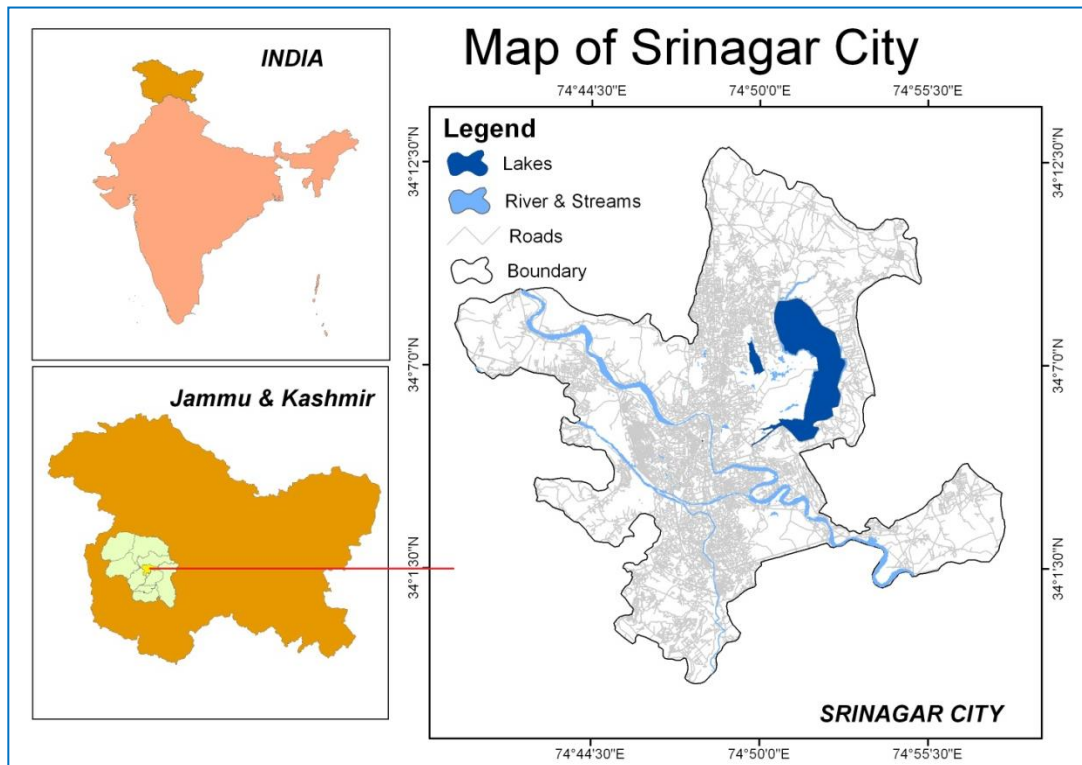


Fig 1 study area.

**Methodology:** LANDSAT 8 data was used in this analysis to identify different LST with the help of the OLI and TIR sensors. With a 30 m spatial resolution and an additional panchromatic band of 15 m resolution, the OLI sensor delivers eight bands on the visible, near-infrared and shortwave electromagnetic spectrum. At 100 m spatial resolution, the TIRS detects thermal infrared (TIR) radiance with two bands in the atmospheric window between 10 and 12  $\mu\text{m}$ . The band designations of Landsat 8 .Split – window algorithm method was employed to find out LST in the study area. Vegetation proportion calculation, emissivity calculation, LST calculation etc were executed in Arcgis 10.2 software platform. Landsat 8 TIRS and OLI images with Meta data (MTL) file for the study area (Path/Row – 149 / 36) downloaded from Earth Explorer website. The images were already rectified to WGS-1984-UTM-Zone\_43N.

**Split-Window Algorithm:** The split-window algorithm proposed by based on two TIR bands typically located in the atmospheric window between 10 and 12  $\mu\text{m}$ . The mathematical structure of SW algorithm is given as:

$$T_s = T_i + c_1 (T_i - T_j) + c_2 (T_i - T_j)^2 + c_0 + (c_3 + c_4W) (1 - \epsilon) - (c_5 + c_6W) \Delta\epsilon \dots \dots \dots \text{eqn.1}$$

Where  $T_i$  and  $T_j$  are the at-sensor brightness temperatures of bands  $i$  and  $j$  is the mean emissivity, and given by  $\epsilon = 0.5 (\epsilon_i + \epsilon_j)$ ,  $\Delta\epsilon$  is the emissivity difference,  $\Delta\epsilon = (\epsilon_i - \epsilon_j)$ ,  $W$  is the total atmospheric water vapour content (in  $\text{gcm}^{-2}$ ), and  $(c_0 - c_6)$  are the SW

coefficients. The basic inputs to SW algorithm are brightness temperature and Land Surface Emissivity LSE. Detailed description of the methodology is outlined here.

Step1: Top of Atmosphere (TOA) Radiance:

Using the radiance rescaling factor, Thermal Infra-Red Digital Numbers can be converted to TOA spectral radiance.

$$L\lambda = M_L Q_{cal} + A_L \dots \dots \dots \text{eqn. 2}$$

Where:

- $L\lambda$  = TOA spectral radiance (Watts / (m<sup>2</sup> \* sr \* μm))
- $M_L$  = Radiance multiplicative Band (No.)
- $A_L$  = Radiance Add Band (No.)
- $Q_{cal}$  = Quantized and calibrated standard product pixel values (DN)

Step 2: Correcting the Reflectance value with the sun angle Reflectance with a correction for the sun angle is then:

$$\rho\lambda = \frac{\rho\lambda'}{\cos\theta_{SZ}} = \frac{\rho\lambda'}{\sin\theta_{SE}} \dots \dots \dots \text{eqn. 3}$$

Where:

- $\rho\lambda$  = TOA planetary reflectance,
- $\theta_{SE}$  = Local sun elevation angle.
- The scene centre sun elevation angle in degrees is provided in the metadata
- $\theta_{SZ}$  = Local solar zenith angle;
- $\theta_{SZ} = 90^\circ - \theta_{SE}$ .

Step 3 Top of Atmosphere (TOA) Brightness Temperature:

Spectral radiance data can be converted to top of atmosphere brightness temperature using the thermal constant Values in Meta data file.

$$BT = \frac{K_2}{\ln\left(\frac{K_1}{L\lambda+1}\right) - 272.15} \dots \dots \dots \text{eqn. 4}$$

Where:

- BT = Top of atmosphere brightness temperature (°C)
- $L\lambda$  = TOA spectral radiance (Watts/ ( m<sup>2</sup> \* sr \* μm))
- $K_1$  = K1 Constant Band (No.)
- $K_2$  = K2 Constant Band (No.)

Step 4: Normalized Differential Vegetation Index (NDVI):

The Normalized Differential Vegetation Index (NDVI) is a standardized vegetation index which Calculated using Near Infra-red (Band 5) and Red (Band 4) bands

$$NDVI = \frac{NIR(B5) - RED(B4)}{NIR(B5) + RED(B4)} \dots \dots \dots eqn. 5$$

Where:

- RED= DN values from the RED band ,
- NIR= DN values from Near-Infrared band

Step 5

$$PV = \left[ \frac{NDVI - NDVI_{min}}{NDVI - NDVI_{max}} \right] \Lambda 2 \dots \dots \dots eqn. 6$$

Now we can get PROPVEG as an output of Proportion of vegetation.

Where:

- PV = Proportion of Vegetation
- NDVI = DN values from NDVI Image
- NDVI<sub>min</sub> = Minimum DN values from NDVI Image
- NDVI<sub>max</sub> = Maximum DN values from NDVI Image

The PV is generally defined as the ratio of the vertical projectionarea of vegetation (including leaves, stalks, and branches)

Step 6

Land Surface Emissivity (LSE):

Land surface emissivity (LSE) is the average emissivity of an element of the surface of the Earth calculated from NDVI values

$$E = 0.004 * PV + 0.986 \dots \dots \dots eqn. 7$$

Now we can calculate LSE by applying Pv value in equation 6

Where:

- E = Land Surface Emissivity
- PV = Proportion of Vegetation

Step7: Land Surface Temperature (LST):

The Land Surface Temperature (LST) is the temperature which calculated using Top of atmosphere brightness temperature, Wavelength of emitted radiance, Land Surface Emissivity.

$$LST = \frac{BT}{1 + W * \left( \frac{BT}{p} \right) * \ln(e)} \dots \dots \dots eqn. 8$$

Where:

LST = Land surface temperature (in Kelvin),

BT = At-satellite brightness temperature (in Kelvin),

W = wavelength of emitted radiance, (11.5  $\mu\text{m}$ ),

$P = h * c / s$ , ( $1.438 * 10^{-2} \text{ m K}$ )

where

h = Planck's constant ( $6.626 * 10^{-34} \text{ Js}$ ),

s = Boltzmann constant ( $1.38 * 10^{-23} \text{ J/K}$ ),

c = Velocity of light ( $2.998 * 10^8 \text{ m/s}$ )

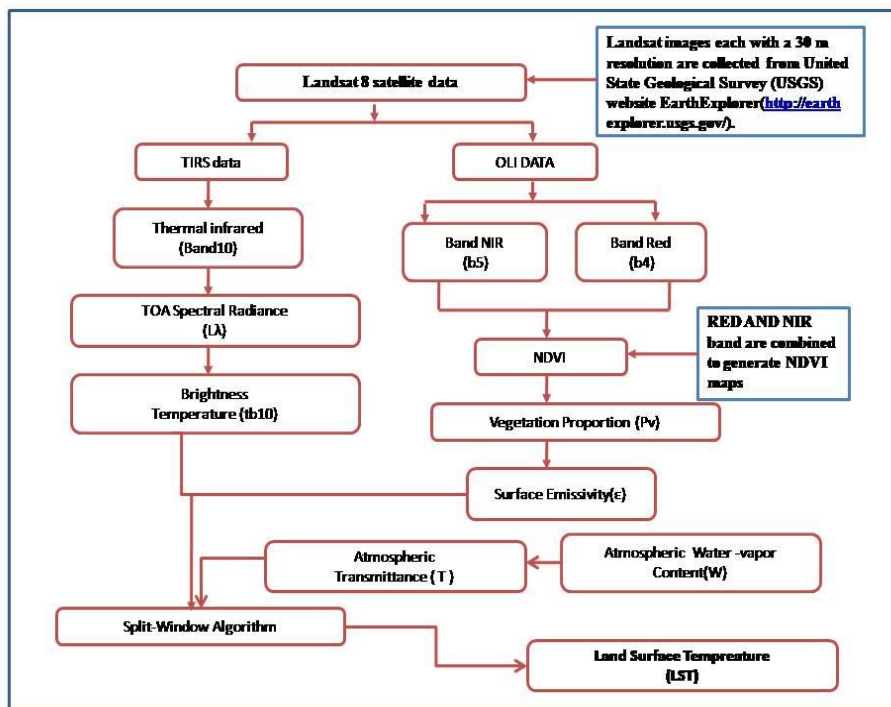


Fig 2. Showing methodology adopted

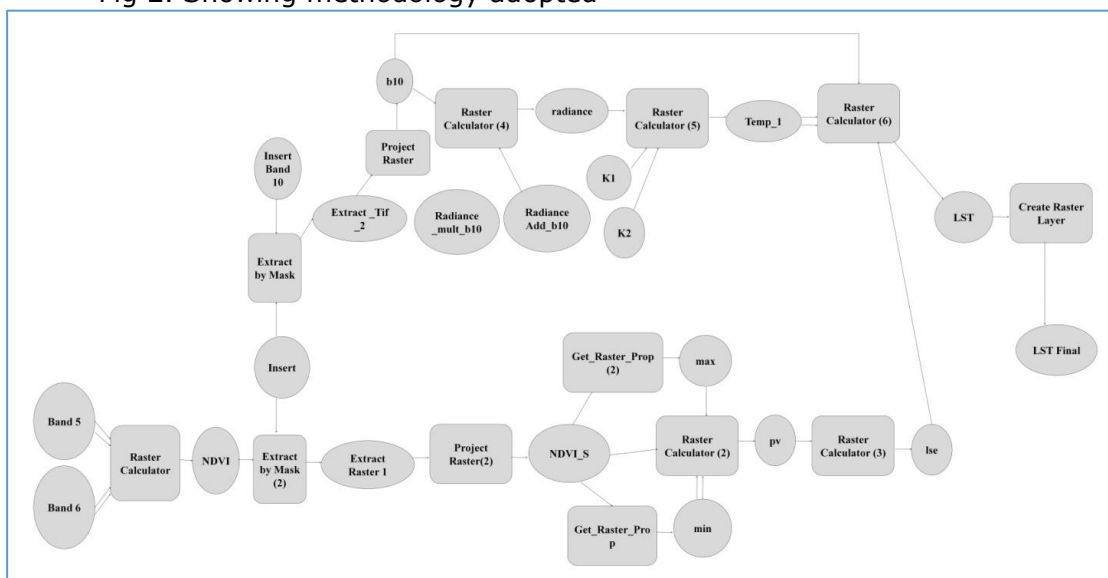


Fig 3. Showing a systematic Diagram of Model Used In the study

Acquisition and selection of data: Landsat 8 TIRS and OLI images with Meta data (MTL) file for the study area (Path/Row - 149 / 36) downloaded from Earth Explorer website. The images were already rectified to WGS-1984-UTM-Zone\_43N. The next step involved is the conversion of DN (Digital Number) to the physical measure of Top of Atmospheric Reflectance (TOA) given in the metadata file and the Thermal band to At-Satellite Brightness Temperature. The file with extension .MTL provided in the Landsat 8 image set contains the thermal constants needed to convert TIRS data to the at-satellite brightness temperature. TIRS band data is used to convert spectral radiance to brightness temperature by processing thermal constants provided in the metadata file (Table.1). The Landsat 8 TIRS sensors acquire temperature data and store this information as a digital number (DN) with a range between 0 and 255.

Table 1 showing satellite data characteristics

		Bands	Wavelength (micrometers)	Resolution (meters)
Landsat and Operational Land Imager(OLI) and Thermal Infrared Sensor (TIRS)		Band I - Coastal Aerosol	0.43 - 0.45	30
		Band 2 - Blue	0.45 - 0.51	30
		Band 3 -Green	0.53 - 0.59	30
		Band 4 - Red	0.64 - 0.67	30
		Band 5 - Near Infrared (NIR)	0.85 - 0.88	30
		Band 6 .SWIR I	1.57 - 1.65	30
		Band 7 - SWIR 2	2.11 - 2.29	30
		Band 8 - Panchro1natic	0.50 - 0.68	15
		Band 9 -Cirru.	1.36 - 1.38	30
		Band 10 -Thennal Infrared (TIRS)	10.60 - 11.19	100 *(30)
		Band II -Thennal Infrared (TIRS)2	11.50 - 12.51	100* (30)



Table 2 showing Metadata of the satellite image

Variable	Description	Values
K1	Thermal constants, band 10	774.8853
K2		1321.0789
Lmax	Maximum and Minimum values of Radiance, Band 10	22.00180
Lmin		0.10033
Qcal <sub>max</sub>	Maximum and Minimum values of Quantize Calibration, Band 10	65535
Qcal <sub>min</sub>		1
Qi	Correction value, Band 10	0.29

### RESULT AND DISCUSSION

Derivation of NDVI: NDVI is a measurement of the surface vegetation index of greenness or photosynthetic activity in a plant. (Singh, P., & Javeed, O. 2020). It is related to vegetation health, since healthy vegetation represents high energy levels. The pixel NDVI values vary from 1 to -1. Higher NDVI values indicate healthy plants while the lower values indicate poor and sparse plants. In the study region the NDVI value ranges from 0.537 to -0.160. (Fig. 4). The study shows that the urban expansion is causing unhealthy and sparse vegetation.

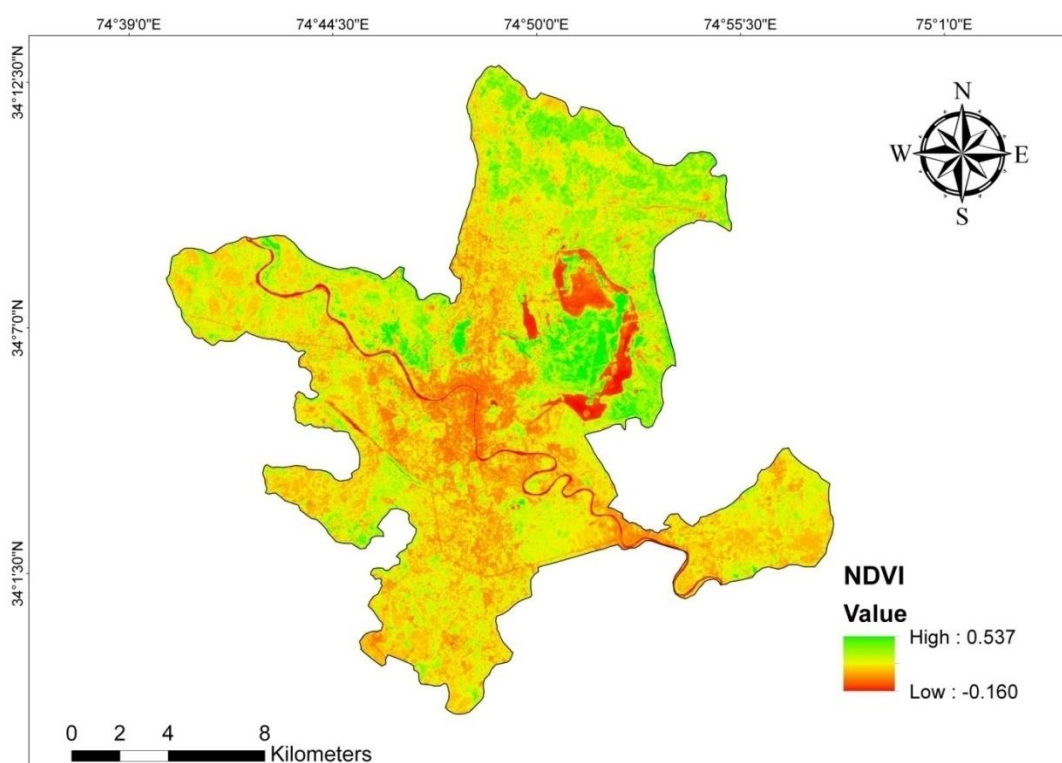


Fig 4. showing NDVI map

Derivation of Emissivity: In this study the emissivity value varies between 0.991 and 0.982 (Fig. 5). In the studied region, emissivity decreases from forest and other vegetational regions due to a drop in surface temperature due to the inverse LSE-LST connection. In addition, it is estimated that the vegetation proportion (PV) in the region of investigation is 0.165-0.947.

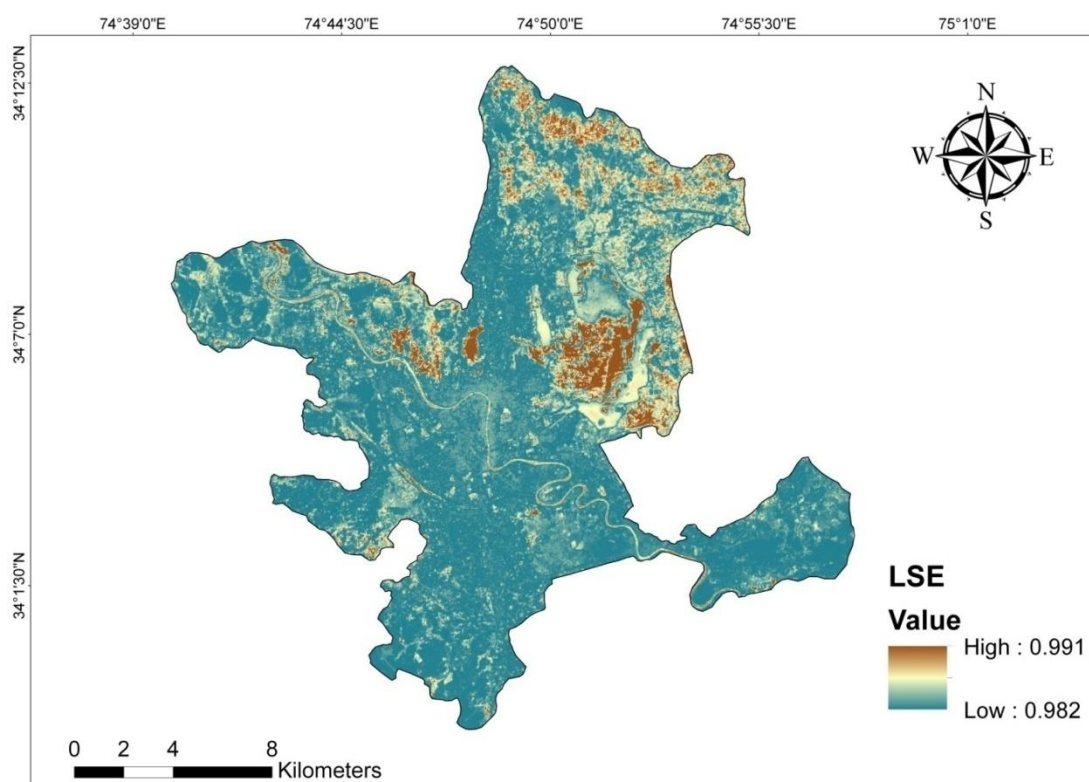


Fig 5.showing Emissivity map

Derivation of LST: LST represents the temperature of an object within a pixel, which may include several land cover types. LST maps are prepared to show the spatial distribution of LST within the study area. The maximum LST was observed as 29.40° C and the minimum LST was observed as 13.09° C in the month of October (Fig.6). The results also show that there are variations in the LST of the area due to variations in the topography of the study area. Also shown variations in barren land and water body coverage. Mean temperature of 19.80°C was observed with a standard deviation of 2.39. we recorded the temperature of dal lake as 15° C on 26-10-2019 at 10.30 a.m. (local standard time) whereas the satellite data-based result shows that the pixels covering the same area have a temperature of 15.447° C.

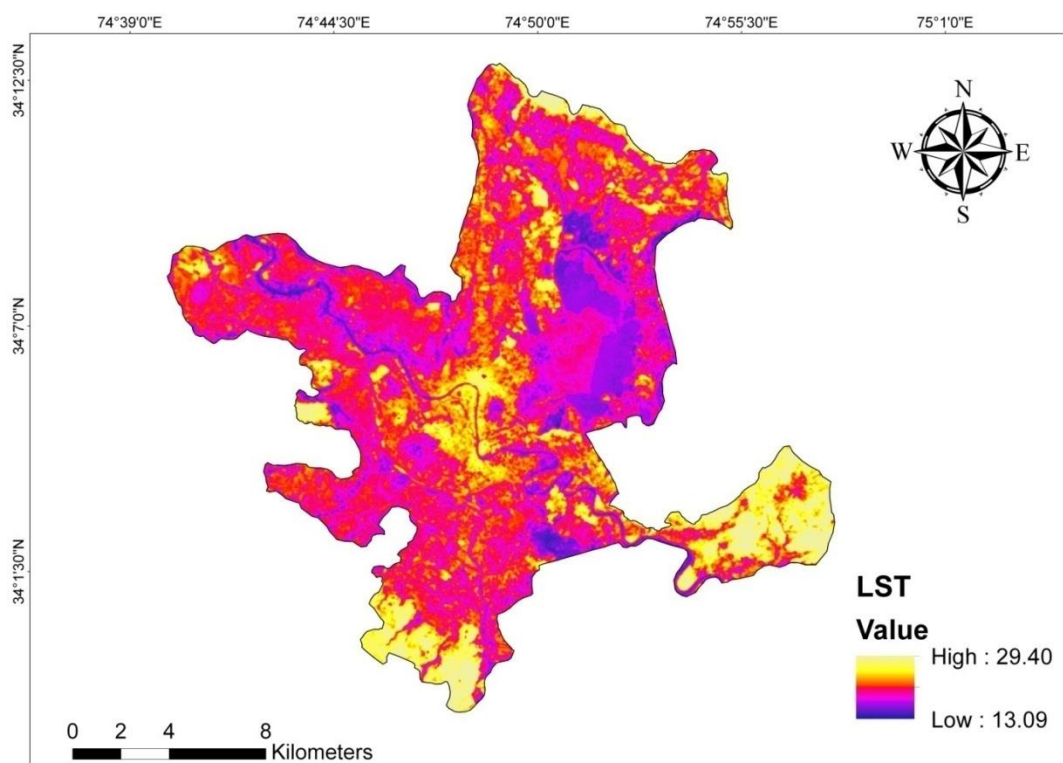


Fig 6. Showing LST map

Table-3: Statistics of Landsat 8 LST Srinagar City

Statistics of Landsat 8 LST	
Sensor	TIRS
Minimum Temperature	13.09
Maximum Temperature	29.40
Mean Temperature	19.80
Standard deviation	2.39

## CONCLUSIONS

In this paper, remote sensing potential is used to evaluate the temperature variation in the city of Srinagar by estimating the LST distribution with the use of Landsat 8 OLI and TIRS Sensor provided by USGS. To compute the LST from the TIRS, Split window algorithm approaches was used. The radiated thermal energy of the earth surface determines the surface temperature variations of the various patterns of surface applications, the plant cover and the soil in the research region. The results also show that there are variations in the LST

of the area due to variations in the topography of the study area. Also shown variations in barren land and water body coverage. Mean temperature of 19.80°C was observed with a standard deviation of 2.39. The variation in surface temperature affects the heat surface and water exchange in the area with the atmosphere that results in climate change. Although certain climate phenomena have a modest influence in temperature fluctuations, the main role, such as land conversion, owing to the fast tourism growth, ever-increasing emissions of motor CO<sub>2</sub> emissions, the burning of fire wood from the kitchen, etc. Remote sensing data like Landsat 8 TIRS have been proven effective in calculating LST. This helps us to evaluate the microclimate, heat pocket and maximum temperature of sensitive places and also to implement the appropriate scientific measures such as forestation, frequent vehicles pollution controls

#### REFERENCES

- Alam, A., Bhat, M.S., Kotlia, B.S., Ahmad, B., Ahmad, S., Taloor, A.K., Ahmad, H.F., 2017. Coexistent pre-existing extensional and subsequent compressional tectonic deformation in the Kashmir basin, NW Himalaya. *Quat. Int.* 444, 201–208
- Anderson MC, Kustas WP, Norman JM, Hain CR, Mecikalski JR, Schultz L, Gonzalez-Dugo MP, Cammalleri C, d'Urso G, Pimstein A, Gao F (2011) Mapping daily evapotranspiration at field to continental scales using geostationary and polar orbiting satellite imagery. *Hydrology and Earth system sciences*, 15 (1): 223-229.
- Arnfield, A. J. (2003). Two decades of urban climate research: a review of turbulence, exchanges of energy and water, and the urban heat island. *International Journal of Climatology: a Journal of the Royal Meteorological Society*, 23(1), 1-26.
- Bastiaanssen, W. G., Menenti, M., Feddes, R. A., & Holtslag, A. A. M. (1998). A remote sensing surface energy balance algorithm for land (SEBAL). 1. Formulation. *Journal of hydrology*, 212, 198-212.
- Fisher, J. B., Melton, F., Middleton, E., Hain, C., Anderson, M., Allen, R., ... & Wood, E. F. (2017). The future of evapotranspiration: Global requirements for ecosystem functioning, carbon and climate feedbacks, agricultural management, and water resources. *Water Resources Research*, 53(4), 2618-2626.
- Grigsby SP, Hulley GC, Roberts DA, Scheele C, Ustin SL, Alsina MM (2015) Improved surface temperature estimates with MASTER/AVIRIS sensor fusion. *Remote Sens Environ* 167:53–63. <https://doi.org/10.1016/j.rse.2015.05.019>

Hansen, J., Ruedy, R., Sato, M., & Lo, K. (2010). Global surface temperature change. *Reviews of Geophysics*, 48(4).

Irons JR et al (2012) The next landsat satellite: the landsat data continuity mission. *Remote Sens Environ* 122:11–21, doi:10.1016/j.rse.2011.08.026

Jin, M., Liang, S., 2006. An improved land surface emissivity parameter for land surfacemodels using global remote sensing observations. *J. Clim.* 19 (12), 2867–2881

Kalma, J. D., McVicar, T. R., & McCabe, M. F. (2008). Estimating land surface evaporation: A review of methods using remotely sensed surface temperature data. *Surveys in Geophysics*, 29(4-5), 421-469.

Kannaujiya, S., Gautam, P.K.R., Chauhan, P., Roy, P.N.S., Pal, S.K., Taloor, A.K., 2020. Contribution of seasonal hydrological loading in the variation of seismicity and geodetic deformation in Garhwal region of Northwest Himalaya. *Quat. Int.* <https://doi.org/10.1016/j.quaint.2020.04.049>.

Kogan, F. N. (2001). Operational space technology for global vegetation assessment. *Bulletin of the American meteorological society*, 82(9), 1949-1964.

Kothyari, G.C., Joshi, N., Taloor, A.K., Kandregula, R.S., Kotlia, B.S., Pant, C.C., Singh, R.K., 2019. Landscape evolution and deduction of surface deformation in the Soan Dun, NW Himalaya, India. *Quat. Int.* 507, 302–323

Liang, X.Z., Xu, M., Yuan, X., Ling, T., Choi, H.I., Zhang, F., Chen, L., Liu, S., Su, S., Qiao, F., He, Y., 2012. Regional climate–weather research and forecasting model. *Bull. Am. Meteorol. Soc.* 93 (9), 1363–1387

Liu Y, Hiyama T, Yamaguchi Y (2006) Scaling of land surface temperature using satellite data: a case examination on ASTER and MODIS products over a heterogeneous terrain area. *Remote Sens Environ* 105(2):115–128. <https://doi.org/10.1016/j.rse.2006.06.012>

Mahmood R, Pielke Sr RA, Hubbard KG, Niyogi D, Bonan G, et al. (2010) Impacts of land use/land cover change on climate and future research priorities. *Bulletin of the American Meteorological Society* 91: 37-46.

Malik, M.S., Shukla, J.P., 2018. Retrieving of land surface temperature using thermal remote sensing and GIS techniques in Kandaihimmat watershed, Hoshangabad, Madhya Pradesh. *J. Geol. Soc. India* 92 (3), 298–304

Mallick J, Kant Y, Bharath BD (2008) Estimation of land surface temperature over Delhi using Landsat and ETM. *J Indian Geophys Union* 12(3):131–140

- Niclos, R., Valiente, J.A., Barbera, M.J., Estrela, M.J., Galve, J.M., Caselles, V., 2009. Preliminary results on the retrieval of land surface temperature from MSG-SEVIRI data in Eastern Spain. In: EUMETSAT 2009: Proceedings of Meteorological Satellite Conference, pp. 21–25.
- Pu, R., Gong, P., Michishita, R., Sasagawa, T., 2006. Assessment of multi-resolution and multi-sensor data for urban surface temperature retrieval. *Remote Sens. Environ.* 104, 211–225
- Rajeshwari A and Mani ND (2014), "Estimation of Land Surface Temperature of Dindigul District using Landsat 8 Data", *IJRET: International Journal of Research in Engineering and Technology*, Vol.03, Issue.05
- Singh, P., & Javeed, O. (2020). NDVI Based Assessment of Land Cover Changes Using Remote Sensing and GIS (A case study of Srinagar district, Kashmir). *Sustainability, Agri, Food and Environmental Research*
- Singh, S., Sood, V., Taloor, A.K., Prashar, S., Kaur, R., 2020. Qualitative and quantitative analysis of topographically derived CVA algorithms using MODIS and Landsat-8 data over Western Himalayas, India. *Quat. Int.* <https://doi.org/10.1016/j.quaint.2020.04.048>
- Tan KC, San Lim H, MatJafri MZ, Abdullah K (2010) Landsat data to evaluate urban expansion and determine land use/land cover changes in Penang Island, Malaysia. *Environ Earth Sci* 60(7):1509–1521. <https://doi.org/10.1007/s12665-009-0286-z>
- Voogt, J. A., & Oke, T. R. (2003). Thermal remote sensing of urban climates. *Remote sensing of environment*, 86(3), 370-384.
- Weng, Q., Lu, D., & Schubring, J. (2004). Estimation of land surface temperature–vegetation abundance relationship for urban heat island studies. *Remote sensing of Environment*, 89(4), 467-483.
- Weng, Q. (2009). Thermal infrared remote sensing for urban climate and environmental studies: Methods, applications, and trends. *ISPRS Journal of Photogrammetry and Remote Sensing*, 64(4), 335-344.
- Xiong, Y., Huang, S., Chen, F., Ye, H., Wang, C., & Zhu, C. (2012). The impacts of rapid urbanization on the thermal environment: A remote sensing study of Guangzhou, South China. *Remote sensing*, 4(7), 2033-2056.

Sustainability, Agri, Food and Environmental Research, (ISSN: 0719-3726), 12(X), 202X:  
<http://dx.doi.org/10.7770/safer-V12N1-art2573>

Van De Griend, A.A., Owe, M., 1993. On the relationship between thermal emissivity and the normalized difference vegetation index for nature surfaces. *Int. J. Rem. Sens.* 14,1119–1131.

Received: 24<sup>th</sup> May 2021; Accepted: 07<sup>th</sup> Jule 2021; First distribution: 22<sup>th</sup> March 2022.